Interparticle coupling effects in surface-enhanced Raman scattering

Hongxing Xu, Erik J. Bjerneld, Javier Aizpurua, Peter Apell, Linda Gunnarsson, Sarunas Petronis,
Bengt Kasemo, Charlotte Larsson, Fredrik Höök, and Mikael Käll*
Dep. of Applied Physics, Chalmers Univ. of Technology, S-412 96 Göteborg, Sweden

ABSTRACT

We report experimental and theoretical results on the effect of electromagnetic coupling between metal particles in surface-enhanced Raman scattering (SERS). Model calculations of the near-field optical properties of Ag and Au nanoparticle-aggregates show that the electromagnetic surface-enhancement factor can reach 11 orders-of-magnitude in gaps between nearly touching particles. Single particles exhibit a much weaker enhancement, unless the particles contain extremely sharp surface protrusions. Data on spectral fluctuations in single-molecule SERS and measurements on the efficiency of nanofabricated SERS substrates give experimental support for the idea that an efficient interparticle coupling is a necessary requirement for an ultra-high surface-enhancement. We suggest a route for biorecognition induced coupling of metal particles for use in biosensing applications.

- nanoparticles, surface-enhanced Raman scattering, Mie theory, biosensors

1. INTRODUCTION

The spectacular optical effects associated with systems of metallic nanoparticles have fascinated scientists and laymen alike for centuries [1]. These properties are due to collective electron-photon resonances (surface plasmon polaritons) in the confined geometry defined by the size and shape of the nanoparticle. The optical properties thus vary with particle morphology, as well as with the dielectric properties of the particle itself and the medium immediately surrounding it. If several particles are close together, the single-particle resonances couple and the optical properties change. A prototypical example of a far-field interparticle coupling effect is the color change of a gold hydrosol upon aggregation, a phenomenon that has been used e.g. for the recent realization of an ultrasensitive polynucleotide optical detection method [2].

Surface-enhanced spectroscopies, such as surface-enhanced Raman scattering (SERS), rely on the near-field optical properties of metal nanoparticles or nanostructures, in particular on the increase in the electromagnetic field strength that occurs close to the metal particle surface when a collective resonance is excited. It is well known that aggregation effects can increase the SERS efficiency of colloidal nanoparticle systems substantially, indicating the importance of interparticle coupling effects for the surface-enhancement [3,4]. However, recent SERS reports on enormous enhancement-factors (14-15 orders-of-magnitude) and single-molecule detection efficiency [5] have caused a renewed interest into the basic mechanisms and requirements of SERS. This presentation, which is based on ref. [6-11], summarizes some of our work on SERS with a focus on electromagnetic coupling between metal particles.

2. MODELLING INTERPARTICLE COUPLING EFFECTS IN SERS

Consider an electromagnetic field E_0 interacting with a small metal sphere of radius a and complex dielectric function $\varepsilon(\omega)=\varepsilon_1(\omega)+i\varepsilon_2(\omega)$ embedded in a uniform medium of dielectric constant ε_m. In the Rayleigh size-regime ($a<<\lambda$), we can treat the incident field as a plane wave. The induced dipole moment P in the sphere will be directed along the incident polarization vector and have a magnitude:

$$P = \varepsilon_m \alpha E_0 = 4\pi\varepsilon_0\varepsilon_m \frac{\varepsilon - \varepsilon_m}{\varepsilon + 2\varepsilon_m} a^3 E_0 \tag{1}$$

A surface-plasmon resonance occurs when $\varepsilon+2\varepsilon_m = 0$, which for the case of Ag in air happens at a wavelength of around 380 nm ($\varepsilon \approx -2 + i0.2$). The local field at a distance r from the center of the sphere, in a direction parallel to the incident polarization, will be a sum of the incident field and the induced field from the dipole: $E_{loc} = E_0 + P/2\pi\varepsilon_0 r^3$. A molecule positioned at r will thus experience a "driving" field E_{loc} that is higher than the original field E_0, especially when the incident wavelength coincides with the surface-plasmon resonance. Similarly, a Raman scattered field, emitted by the molecule at r, can reach a detector either directly or via elastic scattering off the metal sphere. These two effects combined constitute the essence of the "classical" electromagnetic theory of SERS. Furthermore, if a complete "symmetry" between the excitation and the emission channel in the Raman scattering process is assumed, the net effect of the presence of the sphere will be an enhancement of the apparent Raman scattering cross-section by a factor:

$$M = \left[\frac{|E_{loc}(\omega_L)|}{|E_0(\omega_L)|}\right]^2 \left[\frac{|E_{loc}(\omega_L - \omega_v)|}{|E_0(\omega_L - \omega_v)|}\right]^2 \qquad (2)$$

where ω_L is the incident (laser) frequency and ω_v is a vibrational frequency of the molecule. The assumptions behind eq. 2, which have been discussed in detail in [3,4], include for example a completely isotropic molecular polarizability tensor. Eq. 2 thus gives an estimated upper limit for the "classical" surface-enhancement. This limit should be the relevant quantity for models of electromagnetic contributions to single-molecule sensitivity in SERS, as outlined in [6]. Note that if the vibrational frequency is assumed much smaller than the laser frequency, then the enhancement factor scales as the *fourth power* of the local field. It is also interesting to note that the enhancement factor for surface-enhanced *fluorescence* is similar to eq. 2, but with the second part replaced by a factor that for example takes into account non-radiative energy transfer to the metal sphere (i.e. fluorescence quenching) [12].
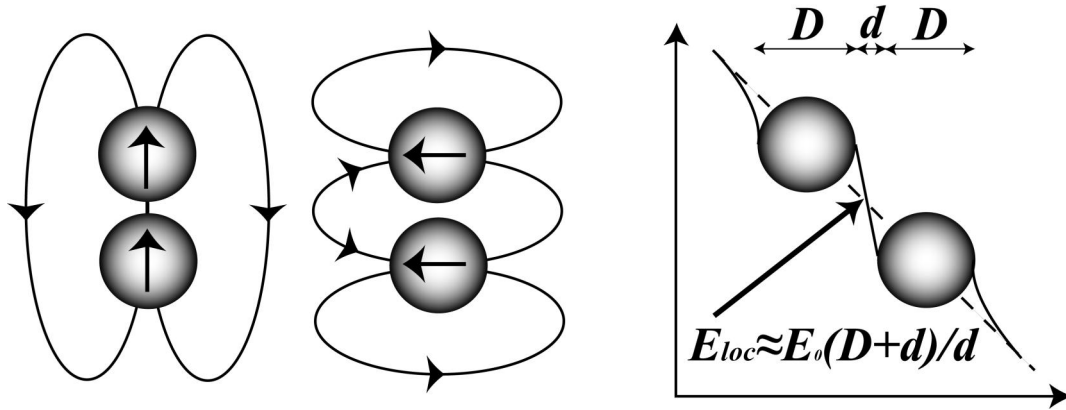

Figure 1: Illustration of electromagnetic coupling between metal particles. An electromagnetic field that interacts with a two-particle system induces two in-phase dipole-moments that reinforce each other if the field is polarized parallel to the main symmetry axis (left) or weaken each other in the perpendicular polarization configuration (center). The coupled-particle surface-plasmon resonances corresponding to these two cases will be red-shifted and blue-shifted, respectively, compared to the single-particle resonance. The figure to the right illustrates the increase of the local field in the interparticle region that occurs for the parallel polarization configuration. Two perfectly conducting particles of diameter D are situated in an electrostatic field of strength E_0. The electrostatic potential drop will be concentrated to the interparticle region of length d, leading to a large increase in the local field for $D/d \gg 1$.

If we now have an "aggregate" of two spheres of radii a_i and a_j separated by a surface-to-surface gap d, an electric field will induce two *in-phase* dipoles oriented along the incident polarization. The induced dipole moment of sphere i in the presence of sphere j now becomes:

$$P_i^* = P_i \frac{1 + c\alpha_j}{1 - c^2 \alpha_i \alpha_j} \ , \qquad i,j = 1,2 \ , \qquad c = \frac{\gamma}{4\pi\varepsilon_0 (d + a_1 + a_2)^3} \qquad (3)$$

where $\alpha_{i,j}$ and $P_{i,j}$ refer to the isolated spheres (eq.1), and $\gamma = -1, 2$ for the perpendicular / parallel polarization configurations shown schematically in Fig.1. The resonance positions of the two modes, determined by $1 - c^2 \alpha_i \alpha_j = 0$, will be blue-shifted and red-shifted, respectively, compared to the single sphere resonances. From Fig. 1 we see that, depending on the angle between the polarization and the "dimer-axis", the two dipoles will either strengthen or weaken each-other. Specifically, the induced field *between* the spheres will be dramatically enhanced in the longitudinal polarization configuration. We can make a rough estimate of this effect through a simple electrostatic model, as shown in the right part of Fig. 1. Imagine two particles of diameter D separated by a distance d and arranged with the "dimer-axis" parallel to a uniform electrostatic field E_0. If the particles are perfectly conducting, the electrostatic potential drop will be concentrated to the interparticle region, resulting in a local field $E_{loc} = E_0 (D+d)/d$ obtained from simple geometrical considerations. A molecule situated between the particles thus experiences a SERS enhancement-factor of the order $M = (D/d + 1)^4$, which in general is much higher than what is obtained for a single particle. The simple electrostatic picture can also be used to estimate the *volume* that is affected by the interparticle coupling. For spherical particles one obtains $V \propto d^2 D$, which for small separation distances can be of nanometric dimensions [6].

The simplistic discussion above illustrates the main effects of interparticle coupling in SERS, namely a shift in plasmon resonance positions and a polarization dependent increase of the enhancement factor in a highly localized region between particles. However, in order to make quantitative predictions it is necessary to perform more advanced calculations. We have utilized Generalized Mie Theory following the calculational procedure described by Inoue and Ohtaka [13] for the case of spherical particles. GMT yields an essentially exact solution to Maxwell's equations for the chosen configuration, including retardation effects and contributions from multipolar resonances. The importance of going beyond the dipole approximation in the case of strongly interacting particles is illustrated in Fig.2. The method allows us to calculate e.g SERS excitation profiles, based on eq. 2, and extinction spectra for linear aggregates of spherical particles of arbitrary sizes and composition and with spherical surface layers of arbitrary thickness and refractive index. A simple example is given in Fig. 3, which shows the variation in the SERS enhancement factor with interparticle separation distance for a system of two interacting Ag spheres in air. The most surprising result in Fig. 3 is perhaps that the simple electrostatic model $M = (D/d + 1)^4$ gives an excellent *quantitative* estimate of the interparticle coupling effect. We refer the reader to ref. [6] for further details and calculations, including wavelength dependencies.
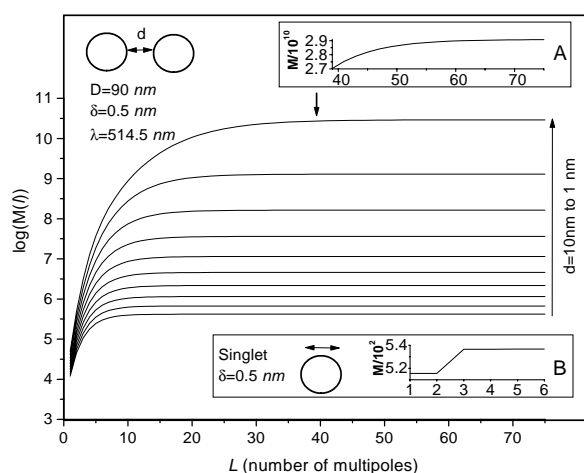

Figure 2: Illustration of multipolar effects in SERS. The figure shows the calculated SERS enhancement-factor, approximated as $M = |E_{loc}/E_0|^4$, for two Ag spheres of diameter $D = 90$ nm separated by a gap d as a function of the number of multipolar terms L that are included in the calculation. The calculations have been performed for the parallel polarization configuration at $\lambda = 514.5$ nm and at a gap-position δ located 0.5 nm outside one of the surfaces along the dimer axis. As shown in inset A, more than 50 multipolar terms are needed for convergence at the smallest interparticle distance. In contrast, the dipole approximation ($L=1$) gives a good estimate of the enhancement-factor outside an isolated particle, as shown in inset B.

The most serious drawback of the GMT is probably the restriction to spherical particle shapes. The colloidal metal particles used in SERS are actually small crystallites with well-defined facets, as shown in Fig.4. The question is then to what extent sharp edges, surface protrusions etc. affect the near-field optical properties. We analyzed a few non-spherical shapes by the Boundary Charge Method (BMT), excluding retardation effects [6]. An example is given in Fig. 4, which shows the variation in the SERS enhancement-factor in a cross-section through a system of two rotationally symmetric polygons with edge-angles similar to what is observed experimentally. The conclusion from these investigations was that the estimated enhancement-factors for fairly open-angled "crystallite-shaped" particle-dimers did not differ substantially from the spherical case. Both the GMT and the BMT calculations predicted maximum enhancement-factors of the order 10^{11} in narrow gaps between particles, for the right choice of wavelength, polarization and particle size. Only in the case of very sharp surface protrusions did we find a similar level of enhancement for single isolated particles. These results indicate that interparticle coupling gives the dominant contribution to single-molecule sensitivity in SERS.
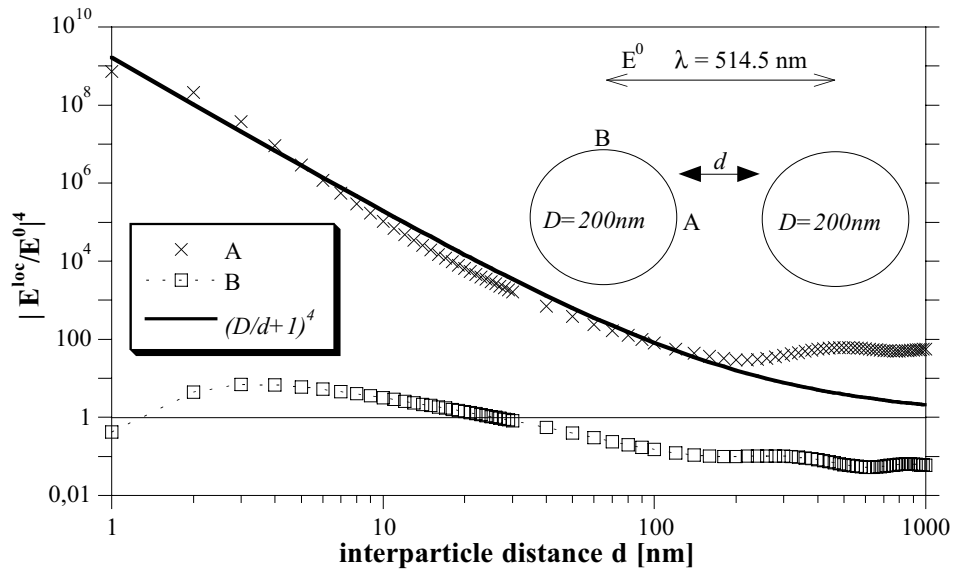
Figure 3: Calculated SERS enhancement-factor for a Ag dimer system in the parallel polarization configuration as a function of interparticle separation *d*. The calculations have been performed for two positions, A and B, located 0.5 nm from the surface of one of the spheres and at λ = 514.5 nm. The electrostatic model of interparticle coupling illustrated in Fig.1 can quantitatively explain the dramatic increase in enhancement that occurs when *D/d* > 1. Note that the enhancement at the off axis position B is almost always below unity (i.e. no enhancement).
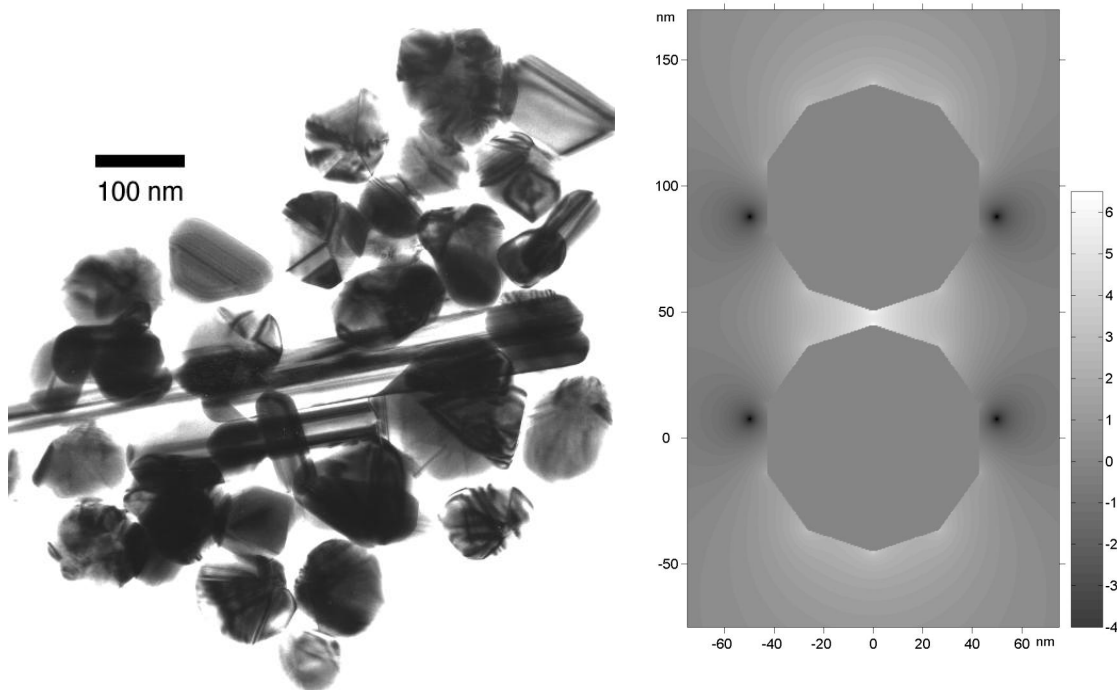

Figure 4: Transmission electron microscopy image of Ag nano-particles (left). This type of particles is found to be efficient substrates for single-molecule SERS [9,10]. Note the heterogeneous distribution of non-spherical shapes. The figure to the right shows the spatial variation of the SERS enhancement-factor in a plane through two interacting rotationally symmetric polygons of largest dimension 90 nm. The interparticle separation is 5.5 nm. The grey-scale gives *M* in orders-of-magnitude on a logarithmic scale. Note the region of high enhancement in the inter-particle region (adapted from ref. [6]).

3. EXPERIMENTAL RESULTS

3.1 Interparticle coupling effects in nanostructured SERS substrates

As noted in the introduction, a large body of experimental results point towards the importance of interparticle coupling effects in SERS. However, for "traditional" SERS systems, such as metal colloids or roughened electrodes, it is very difficult to actually control the degree electromagnetic coupling, as this would imply a tuning of e.g. interparticle separations. This section describes an effort to achieve such control through nanofabrication [7,8].

The technique utilized here is based on electron-beam lithography in conjunction with the so-called lift-off procedure. A resist is spin-coated on an oxidized Si wafer and an electron beam draws the predefined pattern. A developer then removes the exposed resist and a thin metal layer is vapor-deposited on top of the surface. The metal that covers unexposed resist is removed in a suitable solvent ("lift-off"). The manufacturing process is described in greater detail in [8]. The technique allows us to produce uniform arrays of 30-50 nm thick Ag or Au particles in various shapes and with lateral dimensions D down to ~100 nm. The interparticle separation d can be varied *independently* of other parameters down to $d \approx 30$ nm. Fig. 5 shows some examples of the patterns produced.

The efficiencies of the SERS substrates were evaluated by adsorbing a probe-molecule on a sample consisting of a set of 100 μm^2 arrays with different morphology (D, shape) and interparticle separation. The different arrays were then investigated in succession in a notch-filter based single-grating Raman spectrometer equipped with NA=0.95 microscope optics and a CCD detector. All measurements were performed in the back-scattering configuration using the 514.5 nm Ar$^+$-line for excitation. The incident power ranged between 0.2 and 1 mW and the probe-area was 1-2 μm in diameter.

The plot in Fig. 5 shows results obtained for tiophenol adsorbed to arrays of $D = 200$ nm wide square-shaped Ag-particles. It is clear that the relative SERS intensity increases strongly for interparticle separations d below ~100 nm. We analyzed the data with the function:

$$I^{SERS} \propto \frac{A(D/d+1)^4 + B}{(d+D)^2} \qquad (4)$$

where A and B are fitting constants determining the contributions from molecules adsorbed to the particle edges and to the upper particle surfaces, respectively. The former contribution is assumed to vary with particle separation according to the electrostatic model described previously, while the latter is assumed independent of d. These assumptions are motivated by the calculations for spherical particles shown in Fig. 3. The denominator in eq. 4 takes into account the fact that the number of molecules within the probe area varies with d, as tiophenol adsorbs specifically to Ag and not to the Si surface. The best fit to the data set in Fig. 5 is achieved for $B = 0$, indicating a *dominant* interparticle coupling contribution to the overall SERS efficiency in this case. This result illustrates the potential of nanofabrication as a route for controlling and optimizing electromagnetic surface-enhancement effects in optical spectroscopy.
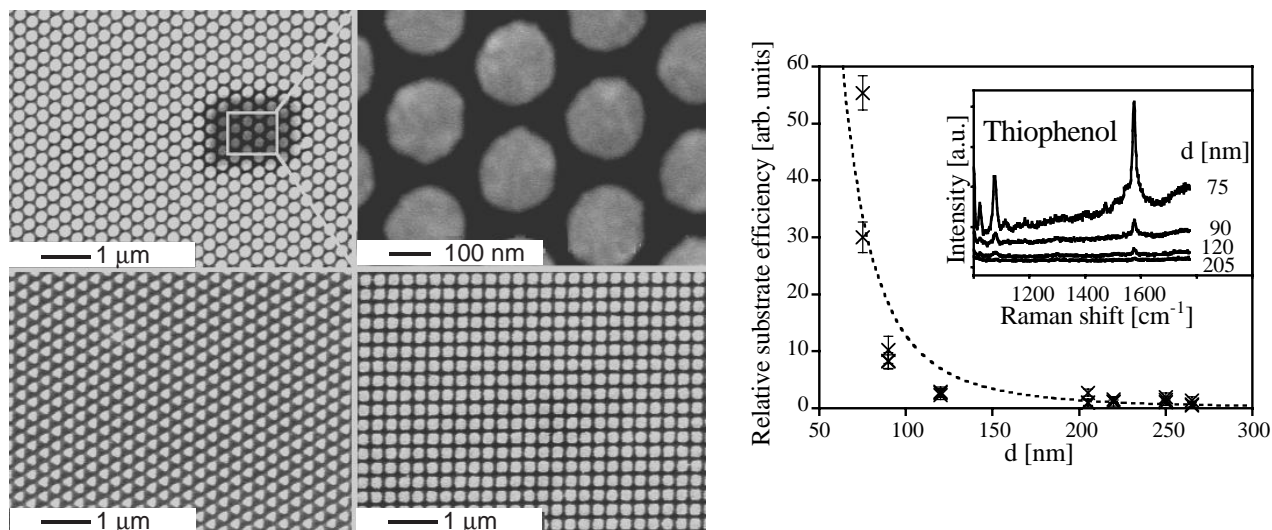

Figure 5: Interparticle coupling effects in SERS substrates prepared by electron-beam lithography (reproduced from ref. [7]) Figure to the left shows scanning electron microscopy images of SERS-substrates consisting of circular, triangular and square 30 nm thin Ag particles on Si. Figure to the right shows the relative SERS-substrate efficiency versus edge-to-edge distance d, quantified as $I^{SERS}(d)/I^{SERS}(d_{max})$, for tiophenol adsorbed to a substrate of square particles of width $D = 200$ nm. Inset shows examples of SERS spectra for different d-values. The dashed line is a single-parameter fit to eq. 4.

3.2 Single-molecule fluctuations as a probe of "hot sites" in SERS

Following the reports by Nie and Emory [14] and Kneipp et al. [15], there has been an increasing interest in SERS as a method for single-molecule detection and spectroscopy. Whereas Kneipp et al. found single-molecule sensitivity for freely diffusing particle clusters in solution, Nie and Emory reported "hot sites" on isolated and immobilized particles. Both groups reported enhancement factors of the order 10^{14}-10^{15}, i.e. at least three orders-of-magnitude higher than the estimated maximum electromagnetic enhancement effect for particle dimers or sharp surface-protrusions [6]. Indications for a dominant interparticle coupling effect in single-molecule SERS came from our study on hemoglobin, for which the "hot sites" corresponded to Ag particle dimers with a size that was close to the calculated optimum dimension at the laser wavelength used [9]. Still, the calculated enhancement factor for the appropriate particle size and separation fell short of the experimental value by about two orders-of-magnitude also in this case. These discrepancies of course raise important questions concerning the origin of single-molecule sensitivity in SERS. This paragraph suggests a somewhat different approach to this problem [10].

The occurrence of spectral fluctuations, i.e. stochastic variations in band positions and intensities, is the perhaps most spectacular "feature" of single-molecule SERS on immobilized particles [9,10]. Although a detailed understanding of this effect is lacking at present, the existence of spectral fluctuations is a strong evidence for extremely localized regions of ultra-high enhancement that effectively block normal ensemble-averaging. An example is given in Fig. 6 A. In this case we have immobilized a monolayer of large Ag-particles ($D \approx 90$ nm) on a substrate and added a *dense* solution of the aromatic amino-acid tyrosine ([Tyr] = 0.1 mM final concentration) in order to occupy as many "hot sites" as possible. Raman measurements were performed with microscope optics as in the previous paragraph. The measurement area ($\Phi \approx 1$-2 μm) thus includes around 100-150 Ag particles. Despite the comparatively large number of particles and the huge number of Tyr molecules present, there are enormous spectral fluctuations indicating a limiting number of "hot sites". In Fig. 6 B, we have repeated the experiment under identical conditions but with *small $D \approx 30$ nm* particles, in which case one expects an order of magnitude more particles within the measurement area. In this case we do *not* observe any spectral fluctuations, indicating a large number of contributing "hot sites". This indicates that the number of probed "hot sites" scale with the average particle size and not with the total Ag area, as would be the case if the "hot sites" were only due to atomic-scale features (e.g. ad-atoms or ion-complexes) or a localized "chemical" enhancement. On the other hand, a mechanism based on electromagnetic enhancement in gaps between particles would predict of the order ~50 and ~500 "hot sites" for the $D = 90$ nm and $D = 30$ nm particle layers, respectively, if approximately half of the gaps were oriented parallel to the incident polarization. This difference would then explain the difference in "ensemble averaging efficiency" for the two cases [10].
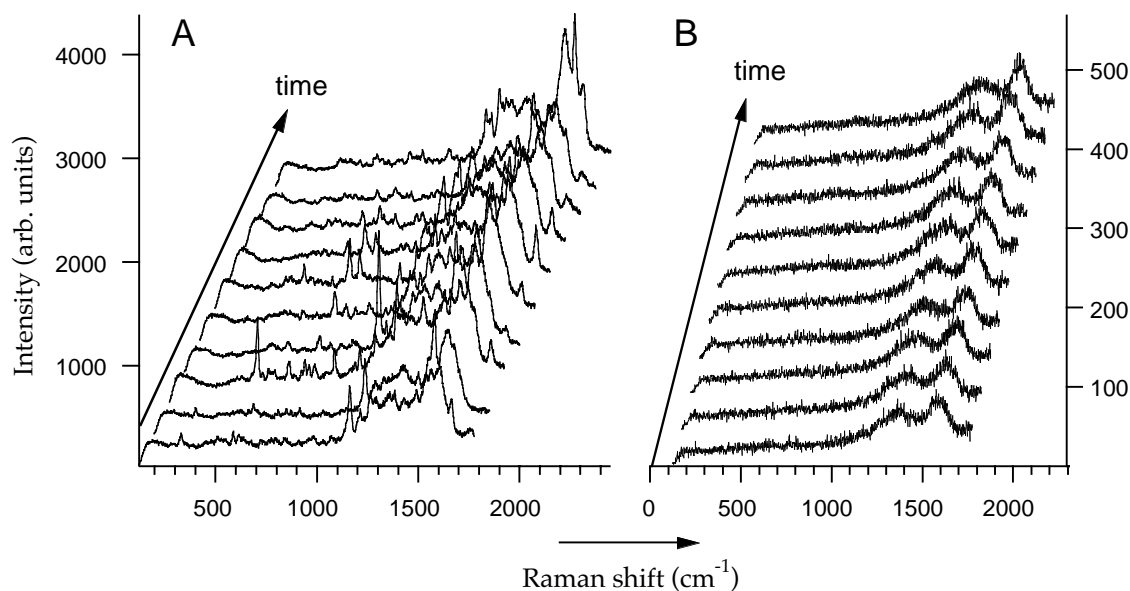

Figure 6: Temporal spectral fluctuations in SERS. **A**: series of consecutive 5-second spectra of tyrosine adsorbed to a layer of 90-nm Ag particles in water. Spectral fluctuations occurred despite the large number of Tyr molecules present in solution (0.1 mM). **B**: same as in A, but for a layer of 30-nm Ag particles. No fluctuations are observed in this case. Except for the particle size, all experimental parameters were the same in the two experiments (laser-power: 2.5 μW, laser spot-size: 1-2 μm, $\lambda = 514.5$ nm). Data adapted from ref. [10].

3.3 Biorecognition induced coupling between metal nanoparticles

In the previous paragraphs, we have presented some theoretical and experimental evidence that indicate that electromagnetic coupling between metal particles is a key-factor in SERS. In colloidal nanoparticle systems, interparticle coupling is achieved through aggregation. This can be induced by disturbing the stability of the colloid, e.g. by adding salt [15] or by adding the probe molecule itself [9]. However, this method is usually too unspecific for analytical purposes. Instead it would be desirable with a highly stable colloid, in which aggregation is induced only by a specific target molecule. This paragraph gives a preliminary account of a method for stabilizing colloidal metal particles and enabling biorecognition-induced coupling through self assembled coating with phospholipids [11].

The main reason for producing lipid-coated nanoparticles is that such a coating would mimic the natural surface properties of living cells, with potential to improve the colloidal stability, and at the same time decrease the influence of the metal surface on the integrity and function of immobilized bio(macro)molecules. It is for example well known that lipid coatings of planar surfaces allow controlled attachment of both transmembrane and water-soluble proteins. Moreover, this method is generic in the sense that a large variety of biological functionalization strategies are available for lipids. Since lipid bilayers do not form spontaneously on neither Au nor Ag, we transferred the procedure to create phosphatidylcholine (PC) lipid monolayers on hydrophobic surfaces to methyl-terminated thiolated metal particles, as illustrated in Fig. 7. We used gold particles with an average diameter of 25 nm. Specific biorecognition induced coupling was induced by incorporating 5% biotinylated lipids in the PC coating followed by addition of streptavidin. A full account of the preparation protocols will be given in a separate publication [11].

The spectra in Fig. 7 illustrate the far-field optical properties of the colloidal systems. The typical extinction spectrum of the bare Au colloid is dominated by the dipolar surface-plasmon resonance at around 525 nm, giving the solution a clear pinkish color. The lipid coated particles exhibit a slightly red-shifted peak-position, induced partly by the change in refractive index of the surface layer and partly by a weak unspecific aggregation. However, addition of streptavidin causes a much more dramatic color change, from bright pink to turbid purple, occurring in a few seconds. This effect is caused by the biorecognition induced formation of *large* nanoparticle clusters that support a set of plasmon resonance pushed far towards the red side of the original dipolar resonance of the isolated Au nanoparticles. We have not yet investigated the SERS characteristics of the present system, but the extinction spectra in Fig. 7 indicate that the enhancement-factor in the 650-800 nm range should increase dramatically due to streptavidin induced aggregation. This may allow for the production of SERS-based biosensors, possibly with sensitivity down to the single-molecule limit.
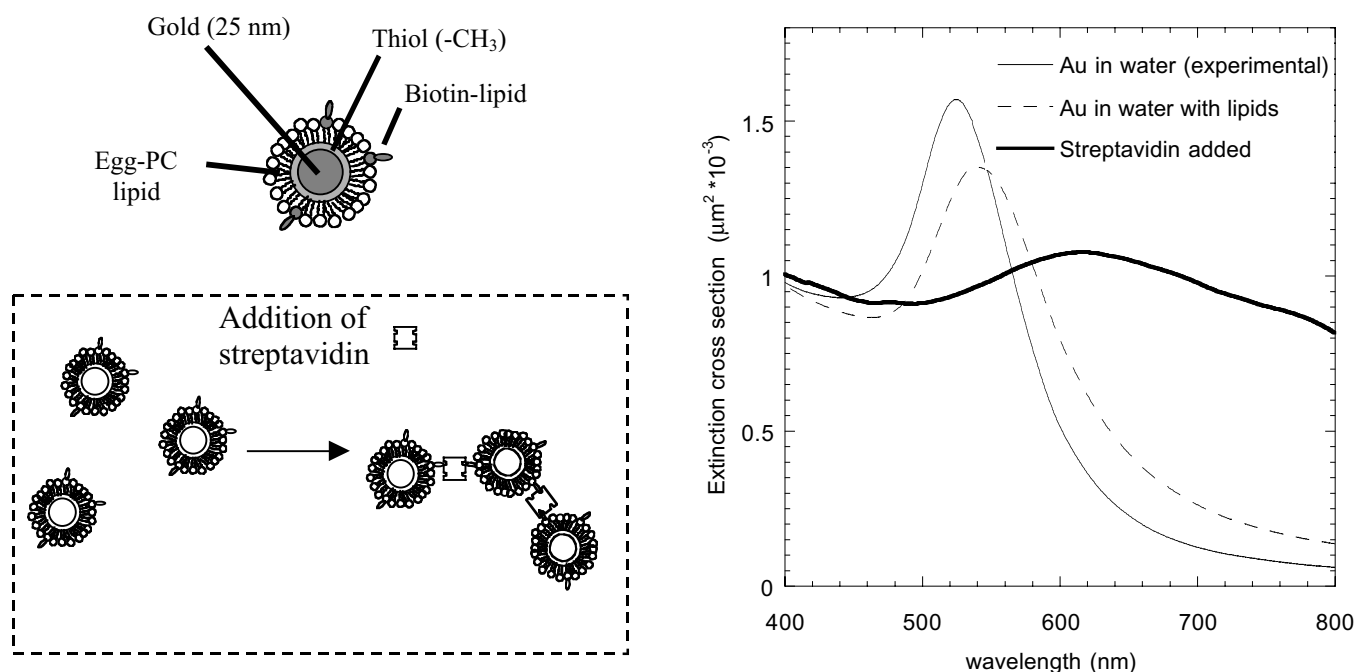

Figure 7: The schematic pictures to the left illustrate the functionalization of Au nanoparticles. The particles are thiolated in order to produce a hydrophobic surface, on which a lipid monolayer can self-assemble. A fraction of the lipids are functionalized by a biotin termination, allowing streptavidin induced aggregation. With slight excess of lipids in the solution, the colloid was sufficiently stable in room temperature for about one week. The figure to the right shows examples of extinction spectra in the visible range. Addition of streptavidin (80 nM final concentration) induces an instant color change from pink to purple.

CONCLUSIONS

Experiments and theory indicate that electromagnetic coupling between metal nanoparticles gives a dominant contribution to the surface-enhanced Raman scattering (SERS) effect, especially in the case of single molecule SERS. Electromagnetic coupling can be achieved in nanofabricated SERS substrates, although the effect is much more efficient in aggregated colloidal systems for which intreparticle distances can be of molecular dimensions. Biorecognition induced coupling of lipid-coated nanoparticles is suggested as a route towards highly efficient SERS-based biosensors.

ACKNOWLEDGEMENTS

REFERENCES

*Corresponding author. E-mail adress: kall@fy.chalmers.se, phone: +46-31-7723119, fax: +46-31-7722090.

[1] U. Kreibig and M. Wollmer, *Optical Properties of Metal Clusters*, Springer Verlag, Berlin 1995.

[2] R. Elghanian, J.J. Storhoff, R.C. Mucic, R.L. Letsinger, and C.A. Mirkin, "Selective colorimetric detection of polynucleotides based on the distance-dependent optical properties of gold nanoparticles", Science **277**, pp. 1078-1081, 1997.

[3] A. Otto, "Surface-enhanced Raman scattering: "classical" and "chemical" origins", in *Light Scattering in Solids IV*, pp. 289-411, edited by M. Cardona and G. Güntherodt, Springer Verlag, Berlin 1984.

[4] M. Moskovits, "Surface-enhanced spectroscopy", Rev. Mod. Phys. 57, pp. 783-826, 1985.

[5] K. Kneipp, H. Kneipp, I. Itzkan, R.R. Dasari, and M.S. Feld, "Ultransensitive chemical analysis by Raman spectroscopy", Chem. Rev. **99**, pp. 2957-2975, 1999.

[6] H. Xu, J. Aizpurua, M. Käll, and P. Apell, "Electromagnetic contributions to single-molecule sensitivity in surface-enhanced Raman scattering", Phys. Rev. E **62**, pp. 4318-4324, 2000.

[7] L. Gunarsson, E.J. Bjerneld, H. Xu, S. Petronis, B. Kasemo, and M. Käll, "Interparticle coupling effects in nanofabricated substrates for Surface-enhanced Raman scattering", Applied Phys. Lett. *to appear*.

[8] L. Gunnarsson, S. Petronis, B. Kasemo, H. Xu, E.J. Bjerneld, and M. Käll, "Optimizing nanofabricated substrates for surface-enhanced Raman scattering", NanoStructured Materials **12**, pp. 783-788, 1999.

[9] H. Xu, E.J. Bjerneld, M. Käll, and L. Börjesson, "Spectroscopy of single hemoglobin molecules by surface-enhanced Raman scattering", Phys. Rev. Lett. **83**, pp. 4357-4360, 1999.

[10] E.J. Bjerneld, P. Johansson, and M. Käll, "Single molecule vibrational fine-structure of tyrosine adsorbed on Ag nano-crystals", Single Molecules **1**, pp. 239-248, 2000.

[11] C. Larsson, H. Xu, M. Käll, and F. Höök, manuscript in preparation.

[12] K. Sokolov, G. Chumanov, and T.M. Cotton, "Enhancement of Molecular Fluorescence near the Surface of Colloidal Metal Films", Anal. Chem. **70**, pp. 3898-3905, 1998.

[13] M. Inoue and K. Ohtaka, "Surface enhanced Raman scattering by metal spheres. I. Cluster effect", J. Phys. Soc. Japan **52**, pp. 3853-3864, 1983.

[14] S.M. Nie and S.R. Emory, "Probing Single Molecules and Single Nanoparticles by Surface-Enhanced Raman-Scattering", Science **275**, pp. 1102-1106, 1997.

[15] K. Kneipp, Y. Wang, H. Kneipp, L.T. Perelman, I. Itzkan, R. R. Dasari, and M.S. Feld, "Single Molecule Detection using Surface-Enhanced Raman Scattering", Phys. Rev. Lett. **78** pp. 1667-1671, 1997.